



Published in final edited form as:

J Magn Reson Imaging. 2015 December ; 42(6): 1656–1665. doi:10.1002/jmri.24929.

Assessment of tumor morphology on diffusion-weighted breast MRI: Diagnostic value of reduced-FOV High resolution DWI

M.W. Barentsz, MD, PhD¹, V. Taviani, PhD², J.M. Chang, MD, PhD³, D.M. Ikeda, MD, PhD², K.K. Miyake, MD, PhD⁴, S. Banerjee, PhD⁵, M.A.A.J van den Bosch, MD, PhD¹, B.A. Hargreaves, PhD², and B.L. Daniel, MD, PhD²

¹Department of Radiology, University Medical Center Utrecht, Utrecht, The Netherlands

²Department of Radiology, Stanford University, Stanford, California, USA ³Department of Radiology, Seoul National University Hospital, Seoul, Korea ⁴Department of Diagnostic Imaging and Nuclear Medicine, Kyoto University Hospital, Kyoto, Japan ⁵Global Applied Science Laboratory, GE Healthcare, Menlo Park, California, USA

Abstract

PURPOSE—To compare the diagnostic value of conventional, bilateral diffusion-weighted imaging (DWI) and high-resolution targeted DWI of known breast lesions.

MATERIALS AND METHODS—Twenty-one consecutive patients with known breast cancer or suspicious breast lesions were scanned with the conventional bilateral DWI technique, a high-resolution, reduced field of view (rFOV) DWI technique and dynamic contrast enhanced MRI (3.0 T). We compared bilateral DWI and rFOV DWI quantitatively by measuring the lesions' ADC values. For qualitative comparison, three dedicated breast radiologists scored image quality and performed lesion interpretation.

RESULTS—In a phantom, ADC values were in good agreement with the reference values. Twenty-one patients (30 lesions: 14 invasive carcinomas, 10 benign lesions (of which 5 cysts), 3 high risk and 3 in situ carcinomas) were included. Cysts and high-risk lesions were excluded from the quantitative analysis. Quantitatively, both bilateral and rFOV DWI measured lower ADC values in invasive tumors than other lesions. In vivo, rFOV DWI gave lower ADC values than bilateral DWI ($1.11 \times 10^{-3} \text{ mm}^2/\text{s}$ vs. $1.24 \times 10^{-3} \text{ mm}^2/\text{s}$, $P=0.002$). ROIs were comparable in size between the two techniques (2.90 vs. 2.13 cm², $P=0.721$). Qualitatively, all three radiologists scored sharpness of rFOV DWI images as significantly higher than bilateral DWI ($P=0.002$). ROC curve analysis showed a higher AUC in BI-RADS classification for rFOV DWI compared to bilateral DWI (0.71 to 0.93 vs. 0.61 to 0.76, respectively).

CONCLUSION—Tumor morphology can be assessed in more detail with high-resolution DWI (rFOV) than with standard bilateral DWI by providing significantly sharper images.

Keywords

Breast cancer; magnetic resonance imaging; diffusion-weighted imaging; tumor morphology

INTRODUCTION

Dynamic contrast-enhanced (DCE) Magnetic Resonance Imaging (MRI) is increasingly being used for the evaluation of suspicious breast lesions and has obtained an important role in clinical practice. Malignant tumors have vascularization patterns that help to differentiate them from benign lesions on contrast enhanced studies [1, 2]. For this purpose, contrast needs to be injected intravenously. Gadolinium contrast can be accompanied with incidental side effects, but occasionally causes serious conditions [3]. Patients with contraindication for Gadolinium contrast may benefit from upcoming techniques which do not require contrast injection. A promising non-invasive MRI technique not requiring intravenous contrast is diffusion-weighted imaging (DWI). DWI assesses the microscopic motion of tissue water molecules, and is thought to reflect cellularity of a lesion and the integrity of cell membranes. Malignant breast lesions demonstrate high cellular density and restricted diffusion of water molecules on DWI, helping to differentiate them from benign breast lesions[4].

Single-shot diffusion-weighted (DW) echo planar imaging (EPI) is the most commonly used technique for DWI due to its insensitivity to motion and high signal-to noise ratio (SNR)[5, 6]. However, DW-EPI suffers from blurring due to T2* decay and is particularly vulnerable to off-resonance due to the narrow effective bandwidth in the phase encode direction. Field inhomogeneities, susceptibility gradients, eddy currents and chemical shift can all lead to artifacts and distortions. For a given field of view (FOV), the amount of blurring and distortion is proportional to the in-plane resolution. For this reason, the typical resolution used for DW bilateral breast exams is about 2mm, which is much less than the <1 mm isotropic resolution afforded by state-of-the-art contrast-enhanced MRI techniques. Higher resolution DWI could allow more accurate characterization of breast lesions by revealing lesion margins and internal features that are important discriminators of malignancy.

Several techniques have been developed for higher resolution DWI that decrease the effective encoded FOV to achieve the desired in-plane resolution while limiting distortion[7–9]. Saritas et al. developed a reduced FOV technique that allows multi-slice, high resolution DWI of targeted volumes without the need for additional outer volume suppression pulses[10]. This technique uses a 2D RF pulse in conjunction with a slice-selective refocusing pulse to limit the FOV in the slice and phase directions while effectively suppressing fat and has been successfully used for imaging the spine[11], the prostate[12] and the breast[13, 14].

Singer *et al.* reported the first results obtained in the breast using this high-resolution, reduced field of view (rFOV) technique at 1.5-T[13]. In eleven patients with locally advanced breast cancer, they found that image quality and lesion depiction was improved with rFOV compared to standard DWI[13].The same method was shown to be superior to

conventional bilateral DWI for monitoring small volumetric changes induced by neoadjuvant chemotherapy in 9 women with advanced breast cancer [14].

The purpose of this study was to assess the diagnostic value of high-resolution rFOV DWI of the breast at 3T by comparing this technique with bilateral DWI and higher resolution contrast-enhanced MRI.

MATERIALS AND METHODS

Imaging was performed on a 3T whole body system (GE Discovery MR750, GE Healthcare, Waukesha, WI) with 50mT/m maximum gradient strength and 200mT/m/s maximum slew rate using a 16-channel bilateral receive-only array coil (Sentinelle Medical, Inc, Toronto, ON, Canada).

Phantom Study

Accuracy of rFOV and bilateral DWI was first evaluated in a prototype breast phantom developed at the National Institute of Standards and Technology (Gaithersburg, USA)[15]. The phantom consisted of several vials containing 10, 25 and 40% PVP (polyvinylpyrrolidone) solutions. The vials were immersed in a mimicking fluid for fibroglandular tissue and positioned 10–12cm off the magnet isocenter. Measurements were performed at 19°C (bore temperature).

The targeted and bilateral DWI pulse sequences were identical (spin echo, single shot) except for the excitation RF pulse and the diffusion-encoding scheme. rFOV DWI used a water-only 2D RF pulse selective in the slice and phase encode directions[10] while bilateral DWI used a water-only, spectral-spatial RF pulse, selective only in the slice direction. A Stajskal-Tanner diffusion-encoding scheme was used for rFOV DWI to minimize the minimum echo time achievable for a given b value due to the intrinsically lower SNR of this technique. For bilateral DWI we used a twice-refocused, eddy-current-compensated diffusion-encoding scheme [16].

The following imaging parameters were used for rFOV DWI: FOV = 10×5cm², slice thickness = 4mm, matrix size = 128×64, number of slices = 16, TE = 61ms, TR = 3s, b = 0, 15, 30, 50, 70, 90, 200, 500, 750 s/mm², number of averages = 8 for b < 200, 16 for b ≥ 200. Diffusion gradients were played on all 3 axes at the same time to achieve the desired b value while minimizing TE. For bilateral DWI we used the same imaging parameters used in our standard clinical protocol: FOV = 32²–34²cm², slice thickness = 5mm, matrix size = 160×160, TE = 78ms, TR = 4s, b = 0, 600 s/mm², number of averages = 8. Diffusion gradients were played on each axis separately and a parallel imaging factor of 4 was used. Both rFOV and bilateral DWI were half Fourier acquisitions with the same effective echo train length so that distortion and blurring due to T2* decay were similar in the 2 cases. rFOV and bilateral DWI gave a true resolution of 0.8×0.8×4mm³ and 2×2×5mm³, respectively. Scan time was 4min. 27s and 4min. 24s for rFOV DWI and bilateral DWI, respectively.

Patient Study Design

Institutional review board approval and written informed consent were obtained. Between June 2013 and February 2014, 21 consecutive patients were enrolled in this prospective study. All patients with previously detected breast cancer or suspicious imaging findings were included. Patients underwent DCE-MRI, bilateral DWI, and rFOV DWI, among other sequences. Exclusion criteria were patients without follow-up or histopathologic confirmation and patients with breast implants.

Data Acquisition

Bilateral and rFOV DWI were performed (in that order) before contrast injection using the same protocol used for the phantom study. The target for the rFOV DWI was determined by examining initial non-contrast T1, T2 and standard DWI for focal abnormalities and marker clips that correspond to previous imaging. Bilateral shimming was performed for bilateral DWI by placing separate shim boxes ($FOV_{\text{shim}} \sim 16\text{cm}$) on each breast. For rFOV DWI, shimming was limited to the target rectangular area.

T1-weighted imaging was performed upon injection of a 0.1 mmol/kg dose of gadobutrol (Gadovist, Bayer Schering Pharma, Pittsburgh, PA, USA). A three-dimensional SPGR (SPoiled Gradient Recalled) acquisition with a variable-density pseudo-random k-space segmentation scheme and Dixon-based fat-suppression (DISCO) provided high spatio-temporal resolution images of the whole breast during the contrast uptake and washout period[17]. The following imaging parameters were used: $FOV = 27^2\text{--}28^2\text{cm}^2$; phase $FOV = 1.2$; slice thickness = 1mm; matrix size = $512 \times 320 \times 188$; true spatial resolution = $0.5 \times 0.8 \times 1\text{mm}^3$; temporal resolution = 8s; $TE1/TE2 = 2.2/3.3\text{ms}$; $TR = 6.3\text{ms}$; receiver bandwidth = 125–167kHz; flip angle = 12° . Only the temporal phase corresponding to the peak of the contrast uptake curve was considered for the purpose of this study.

Image Analysis

Quantitative—The location of the lesion was determined on the post-contrast T1-weighted images. Cysts and high-risk lesions were excluded for the quantitative analyses. Freehand regions of interest (ROI) were drawn delineating the borders of the tumors, including the maximum amount of tissue, while excluding surrounding fibroglandular tissue.

Corresponding lesions were located on the diffusion images and ROIs were drawn manually on both diffusion-weighted sequences separately. This manual contouring was used to overcome mis-registration due to distortions and non-linearities between the two techniques. ROIs on bilateral DWI ($b = 600\text{ s/mm}^2$) and rFOV DWI ($b = 750\text{ s/mm}^2$) were drawn on the slice showing the largest tumor diameter.

ROIs were drawn by MB (three years of breast cancer research experience) using Osirix Medical Image software[18]. *ADC* values were calculated with a commercially available Osirix Plugin (*ADC* Map Calculation, version 1.6). For rFOV DWI, only $b=0$ and $b=750$ were used to compute *ADC*, however the signal decay curve as a function of b value was visually inspected to exclude eventual noise floor effects.

Qualitative—Three dedicated breast radiologists (DI, JC, KM: 26, 6, and 6 years breast imaging experience) independently reviewed all lesions. The images were presented in Osirix. The T1w post-contrast image showing the lesion was presented side by side with the bilateral DWI and rFOV DWI. Bilateral diffusion-weighted images were cropped to match the same FOV of rFOV DWI. Image quality was scored according to five categories for each acquisition technique: sharpness (5 point scale: 1=unsharp to 5=very sharp), residual artifacts/ghosting (4 point scale: 0=no artifacts to 3=severe artifacts, may interfere with diagnostic information), distortion (4 point scale: 0=no distortions to 3=severe distortions, may interfere with diagnostic information), perceived signal to noise ratio (SNR) (4 point scale: 1=poor to 4=excellent), and fat suppression (5 point scale: 1=failed to 5=excellent). Lesion interpretation was classified according to lesion shape (Figure 1) and overall suspicion for cancer (BI-RADS 1–5, American College of Radiology Breast Imaging Reporting and Data System (BI-RADS) classification for cancer)[19]. Lesion interpretation was based on a single acquisition technique.

Statistical Analysis

Boxplots were created for ADC measurements in benign lesions, noninvasive, and invasive carcinomas for bilateral and rFOV DWI. A Bland-Altman plot was compiled to assess the difference in ADC values (standard DWI – rFOV DWI) versus the corresponding mean ADC value. Mean ADC values and ROI sizes for bilateral DWI and rFOV DWI were compared with paired samples T-Test. Receiving Operation Characteristic (ROC) curves were drawn to discriminate between benign and malignant lesions based on ADC values for both bilateral and rFOV DWI.

For the three readers, scores on image quality (i.e. sharpness, artifacts, distortions, signal intensity, and quality of fat suppression) were compared between the two acquisition techniques by means of the Wilcoxon signed-rank test. The ability to predict a malignancy based on the shape of the lesion and overall BI-RADS classification was analyzed using ROC curves. ROC curves were drawn per acquisition technique and per reader and the area under the curve (AUC) was calculated. Interrater agreement and reliability were analyzed according to the Guidelines for Reporting Reliability and Agreement Studies (GRRAS)[20]. Interrater agreement was analyzed for the BI-RADS classification for all three acquisitions (T1w post-contrast, bilateral, and rFOV DWI) and compared between the readers by means of proportion of agreement. Reliability of BI-RADS classification was analyzed using weighted kappa (linear).

All analyses were performed using SPSS version 20.0 (IBM SPSS Statistics, Chicago, IL, USA) or RStudio (version 0.98.501, RStudio Inc). Significant differences were defined as *P* values of 0.05 or less.

RESULTS

Phantom Study

ADC values derived from both rFOV and bilateral DWI were in good agreement with the reference values (Table 1).

Patients And Lesions

The mean age (\pm SD) of patients was 51.3 (\pm 9.1) years (Table 2). Indication for MRI in the majority of patients (15/21, 71.4%) was a histologically proven breast cancer. A total of 30 lesions were found in these patients. For quantitative analyses, cysts and high risk lesions were excluded, resulting in 22 lesions. The mean size of the lesions was 2.99 cm and ranged from 0.6 to 8.5 cm. Histopathology of the 22 lesions showed 14 invasive carcinomas (all invasive ductal carcinoma), 5 benign lesions, and 3 *in situ* carcinomas (Table 2).

Quantitative Image Analyses

The distribution of ADC values for bilateral DWI and rFOV DWI is shown in Figure 2a and categorized per diagnosis. Both bilateral DWI and rFOV DWI measured lower ADC values in invasive tumors than other lesions (in bilateral DWI: 1.44×10^{-3} mm²/s for non-invasive lesions vs. 1.08×10^{-3} mm²/s for invasive carcinomas, $P=0.003$; and in rFOV DWI: 1.25×10^{-3} mm²/s for non-invasive tumors vs. 1.01×10^{-3} mm²/s for invasive carcinomas, $P=0.05$). The mean ADC value for rFOV DWI was significantly lower than for bilateral DWI (1.11 ± 0.32 vs. $1.24 \pm 0.32 \times 10^{-3}$ mm²/s, $P=0.002$) (Figure 2b). Discriminative abilities based on ADC values were similar for bilateral and rFOV DWI with an AUC of 0.79 (95% CI: 0.60–0.98) and 0.82 (95% CI: 0.61–1.00), respectively (Figure 2c). The correlation between the ADC values of both acquisition techniques was strong with an r of 0.85. The size of the ROIs was comparable (2.09 ± 2.73 cm² for bilateral DWI vs. 2.13 ± 3.17 cm² for rFOV DWI, $P=0.721$).

Qualitative Image Analyses

All 30 lesions were included in the qualitative analysis. Sharpness was rated as significantly higher for rFOV DWI compared to bilateral DWI by all three radiologists (Table 3, Figure 3). One reader found significantly less artifacts and distortions present in rFOV DWI. SNR was perceived as higher in rFOV DWI by two readers. Fat suppression scores were better for rFOV DWI. The ROC curve for the shape of the lesion in predicting a malignancy (i.e. *in situ* or invasive carcinoma) had an AUC ranging from 0.74 to 0.91 for rFOV DWI for the three readers. The AUCs for bilateral DWI ranged from 0.67 to 0.75 and from 0.76 to 0.83 for high-resolution post-contrast T1-weighted imaging. The AUCs for predicting breast cancer based on BI-RADS classification ranged from 0.71 to 0.93 for rFOV DWI, from 0.61 to 0.76 for bilateral DWI and from 0.87 to 0.91 for T1w post-contrast images.

The proportion of agreement for post-contrast T1w ranged from 56–82%, from 38–57% for bilateral DWI and 41–59% for rFOV DWI (Table 4). The weighted kappa's for post-contrast T1w ranged from 0.51–0.83, from 0.21–0.50 for bilateral DWI, and 0.32–0.61 for rFOV DWI.

DISCUSSION

This study shows that tumor morphology can be assessed in more detail with high-resolution DWI than with standard bilateral DWI. While ADC values differed between bilateral DWI and rFOV DWI, both techniques could discriminate between benign and malignant lesions.

The ADC values of both bilateral DWI and rFOV DWI were significantly lower for invasive tumors than other lesions and were similar to reported ADC values in the literature[21–26]. Despite the significantly lower ADC values, bilateral DWI and rFOV DWI were equivalent in discriminating between benign and malignant lesions and this difference in ADC has, therefore, little clinical impact as long as the threshold for abnormal ADC values was adjusted. There is not however a clearly established threshold for malignancies and reported thresholds range from 1.10×10^{-3} to 1.6×10^{-3} [22–26]. ADC values in the breast are confounded by multiple factors and comparisons between different studies are difficult due to lack of standardization and the use of different pulse sequences. The ADC values in our study were significantly lower for rFOV DWI than bilateral DWI. Wilmes *et al.* reported a trend towards lower ADC values for high-resolution DWI compared to standard bilateral DWI[14]. They found a statistical significant difference in ADC values when the 15th percentile of high-resolution DWI was compared to the 15th percentile of standard DWI. Singer *et al.* found significant differences in tumor ADC distributions between the two sequences, especially in the low ADC region[13]. Both studies attributed this effect to reduced partial volume averaging with healthy fibroglandular tissue and residual fat in the higher resolution images. This hypothesis is supported by the fact that in our study there was no difference between bilateral DWI and rFOV DWI when ADC measurements were performed in a diffusion phantom with reference ADC values typically found in breast lesions. Our phantom measurements ruled out that eddy currents, concomitant gradients and other system imperfections may have been the cause of the discrepancy found in vivo. Visual inspection of the signal decay curve as a function of b value for rFOV DWI excluded the presence of noise floor effects, which could have explained the observed bias in ADC. While the use of different b values could potentially result in different ADC values depending on the underlying tissue microstructure, it has been shown that in the absence of perfusion effects, the diffusion signal decay is well described by a monoexponential function up to b values $>1000 \text{ s/mm}^2$ [27]. Despite these observations all suggest that reduced partial volume averaging with surrounding non-tumor tissue could be the primary cause for the observed systematic bias in ADC, further studies are needed to confirm or disprove this hypothesis.

The AUC predicting malignancies based on BI-RADS score for rFOV DWI was higher than for bilateral DWI. The additional information on tumor morphology (e.g. lesion shape and borders) provided by rFOV DWI could have contributed to this higher AUC. When only the shape of the lesion was taken into account for lesion interpretation, the AUC for rFOV DWI was higher than for bilateral DWI and similar to T1w post-contrast MRI. Recently, Kang *et al.* also reported on assessing tumor morphology focusing on a high rim signal for improvement of DWI performance. They found a high-signal rim a valuable morphological feature for improving specificity in DWI, showing a specificity of 80.6%[28]. These advancements of assessing tumor morphology with DWI are promising for the future.

rFOV DWI could potentially be used for follow-up of lesions that do not require immediate biopsy or surgical excision. When a breast lesion is found on (contrast-enhanced) MRI and follow-up is required, as suggested for BIRADS 3 lesions [29], follow-up could be performed by means of rFOV DWI. Being able to evaluate tumor morphology with this

sequence, accurate follow-up could be provided without the need for consecutive contrast injections.

The use of rFOV DWI in a clinical setting for follow-up of BI-RADS 3 lesions or during neoadjuvant chemotherapy might also be a cost-effective way to monitor the tumor. MRI is currently being used for evaluation of histopathological response to neoadjuvant chemotherapy [30]. With the high costs of MRIs [31], this way of follow-up can be quite costly. When rFOV DWI could be used, without the need of contrast injection and with favorable scan times, the costs of follow-up by means of MRI can be evidently reduced. While the main objective of this study was to compare each DWI technique separately, in relation to post-contrast T1w, neither technique is likely to be used clinically on its own, except for specific applications such as treatment monitoring or follow-up examinations of known lesions. Further research should therefore focus on establishing the added value of bilateral and/or rFOV diffusion to conventional protocols routinely used in clinical practice. The main limitation of rFOV DWI is the relatively small field-of-view. We performed the diffusion sequences prior to the T1w contrast enhanced sequence, and therefore, it is essential to know the location of the lesion in the breast in order to scan the correct area. For MR screening purposes using DWI, whole breast coverage is necessary and future studies should focus on extending the field-of-view with similar high-resolution images.

This study has several limitations. In addition to having a small sample size, rFOV DWI was added to the standard clinical protocol used at our institution, including, among the other pulse sequences, bilateral DWI. For this reason, while the rFOV DWI protocol was carefully designed to give the best results, both qualitatively and quantitatively, we could not modify the bilateral DWI protocol so that all imaging parameters were matched. While slightly different imaging parameters have minimal effect on qualitative analyses, they could have potentially biased our quantitative results. For this reason, we conducted a series of phantom experiments and analyze the data and ensure that system imperfections and eventual noise floor effects did not produce a systematic bias in ADC. While we provided a possible explanation to the discrepancy between ADC obtained with the two different techniques, more studies are necessary to further investigate this point. Despite the multiple b values available for rFOV DWI, in order to provide the fairest comparison with bilateral DWI, we only used two b values to compute ADC. Similarly, only a single post-contrast phase was analyzed, although several dynamic phases were available. While in this study we decided to focus on diffusion, rather than perfusion effects, further studies are under way to investigate these and other aspects related to the pathophysiology of breast cancer that can be obtained from the data presented here. Another limitation of this study was that the images were presented to the readers side by side. Directly comparing bilateral and rFOV DWI images may have led to a relatively higher quality score for the rFOV images.

In conclusion, tumor morphology can be assessed in more detail with high-resolution DWI (rFOV DWI) than with standard bilateral DWI. While the limited FOV of rFOV DWI requires a known predefined target to be imaged, thus making it unsuitable for screening purposes, these of rFOV DWI in conjunction with conventional bilateral DWI can improve discrimination of benign and malignant lesions as well as provide a more accurate characterization of malignancies.

Acknowledgments

Grants:

NIH R21 EB012591. High resolution 3D diffusion-weighted breast MRI

NIH RO1 EB009055. High-Resolution Whole-Breast MRI at 3.0T.

Disclosures:

S. Banerjee: employee of GE Healthcare (Global Applied Science Laboratory, Menlo Park, CA)

B.A. Hargreaves and B.L. Daniel have research grants from GE Healthcare (Waukesha, WI)

REFERENCES

1. Kaiser WA, Zeitler E. MR imaging of the breast: fast imaging sequences with and without Gd-DTPA. Preliminary observations. *Radiology*. 1989; 170:681–686. [PubMed: 2916021]
2. Kuhl CK, Mielcareck P, Klaschik S, et al. Dynamic breast MR imaging: are signal intensity time course data useful for differential diagnosis of enhancing lesions? *Radiology*. 1999; 211:101–110. [PubMed: 10189459]
3. Yang L, Krefting I, Gorovets A, et al. Nephrogenic systemic fibrosis and class labeling of gadolinium-based contrast agents by the Food and Drug Administration. *Radiology*. 2012; 265:248–253. [PubMed: 22923714]
4. Sinha S, Lucas-Quesada FA, Sinha U, et al. In vivo diffusion-weighted MRI of the breast: potential for lesion characterization. *J Magn Reson Imaging*. 2002; 15:693–704. [PubMed: 12112520]
5. Mansfield P. Multi-planar image-formation using NMR spin echoes. Multi-planar image-formation using NMR spin echoes. *J Phys. C: Solid State Phys*. 1977; 10:L55–L58.
6. Turner R, Lebihan D. Single-Shot Diffusion Imaging at 2.0 Tesla. *J Magn Reson Imaging*. 1990; 86:445–452.
7. Bammer R, Auer M, Keeling SL, et al. Diffusion tensor imaging using single-shot SENSE-EPI. *Magn Reson Med*. 2002; 48:128–136. [PubMed: 12111940]
8. Jeong EK, Kim SE, Guo J, et al. High-resolution DTI with 2D interleaved multislice reduced FOV single-shot diffusion-weighted EPI (2D ss-rFOV-DWEPI). *Magn Reson Med*. 2005; 54:1575–1579. [PubMed: 16254946]
9. Wilm BJ, Svensson J, Henning A, et al. Reduced field-of-view MRI using outer volume suppression for spinal cord diffusion imaging. *Magn Reson Med*. 2007; 57:625–630. [PubMed: 17326167]
10. Saritas EU, Cunningham CH, Lee JH, et al. DWI of the spinal cord with reduced FOV single-shot EPI. *Magn Reson Med*. 2008; 60:468–473. [PubMed: 18666126]
11. Zaharchuk G, Saritas EU, Andre JB, et al. Reduced field-of-view diffusion imaging of the human spinal cord: comparison with conventional single-shot echo-planar imaging. *AJNR Am J Neuroradiol*. 2011; 32:813–820. [PubMed: 21454408]
12. Reischauer C, Wilm BJ, Froehlich JM, et al. High-resolution diffusion tensor imaging of prostate cancer using a reduced FOV technique. *Eur J Radiol*. 2011; 80:e34–e41. [PubMed: 20638208]
13. Singer L, Wilmes LJ, Saritas EU, et al. High-resolution diffusion-weighted magnetic resonance imaging in patients with locally advanced breast cancer. *Acad Radiol*. 2012; 19:526–534. [PubMed: 22197382]
14. Wilmes LJ, McLaughlin RL, Newitt DC, et al. High-resolution diffusion-weighted imaging for monitoring breast cancer treatment response. *Acad Radiol*. 2013; 20:581–589. [PubMed: 23570936]
15. Keenan, KE.; Aliu, SO.; Wilmes, LJ., et al. Universal Breast Phantom for Quantitative MRI. Proceedings of the 22nd Annual Meeting of ISMRM; Milan, Italy. 2014. (abstract 1047).
16. Reese TG, Heid O, Weisskoff RM, Wedeen VJ. Reduction of eddy-current-induced distortion in diffusion MRI using a twice-refocused spin echo. *Magn Reson Med*. 2003; 49:177–182. [PubMed: 12509835]

17. Saranathan M, Rettmann DW, Hargreaves BA, et al. Differential Subsampling with Cartesian Ordering (DISCO): a high spatio-temporal resolution Dixon imaging sequence for multiphase contrast enhanced abdominal imaging. *J Magn Reson Imaging*. 2012; 35:1484–1492. [PubMed: 22334505]
18. Rosset A, Spadola L, Ratib O. OsiriX: an open-source software for navigating in multidimensional DICOM images. *J Digit Imaging*. 2004; 17:205–216. [PubMed: 15534753]
19. Ikeda, DM.; Hylton, NM.; Morris, EA., et al. Illustrated Breast Imaging Reporting and Data System- Magnetic Resonance Imaging (BI-RADS–MRI). Reston: American College of Radiology (ACR); 2003.
20. Kottner J, Audige L, Brorson S, et al. Guidelines for Reporting Reliability and Agreement Studies (GRRAS) were proposed. *J Clin Epidemiol*. 2011; 64:96–106. [PubMed: 21130355]
21. Peters NH, Vincken KL, van den Bosch MA, et al. Quantitative diffusion weighted imaging for differentiation of benign and malignant breast lesions: the influence of the choice of b-values. *J Magn Reson Imaging*. 2010; 31:1100–1105. [PubMed: 20432344]
22. Rubesova E, Grell AS, De Maertelaer V, et al. Quantitative diffusion imaging in breast cancer: a clinical prospective study. *J Magn Reson Imaging*. 2006; 24:319–324. [PubMed: 16786565]
23. Guo Y, Cai YQ, Cai ZL, et al. Differentiation of clinically benign and malignant breast lesions using diffusion-weighted imaging. *J Magn Reson Imaging*. 2002; 16:172–178. [PubMed: 12203765]
24. Hatakenaka M, Soeda H, Yabuuchi H, et al. Apparent diffusion coefficients of breast tumors: clinical application. *Magn Reson Med Sci*. 2008; 7:23–29. [PubMed: 18460845]
25. Marini C, Iacconi C, Giannelli M, et al. Quantitative diffusion-weighted MR imaging in the differential diagnosis of breast lesion. *Eur Radiol*. 2007; 17:2646–2655. [PubMed: 17356840]
26. Woodhams R, Matsunaga K, Kan S, et al. ADC mapping of benign and malignant breast tumors. *Magn Reson Med Sci*. 2005; 4:35–42. [PubMed: 16127252]
27. Clark CA, Le Bihan D. Water diffusion compartmentation and anisotropy at high b values in the human brain. *Magn Reson Med*. 2000; 44(6):852–859. [PubMed: 11108621]
28. Kang BJ, Lipson JA, Planey KR, et al. Rim sign in breast lesions on diffusion-weighted magnetic resonance imaging: Diagnostic accuracy and clinical usefulness. *J Magn Reson Imaging*. 2014 Mar 3. [epub ahead of print].
29. Eby PR, DeMartini WB, Gutierrez RL, et al. Characteristics of probably benign breast MRI lesions. *Am J Roentgenol*. 2009; 193:861–867. [PubMed: 19696303]
30. Warren RM, Bobrow LG, Earl HM, et al. Can breast MRI help in the management of women with breast cancer treated by neoadjuvant chemotherapy? *Br J Cancer*. 2004; 90:1349–1360. [PubMed: 15054453]
31. Esserman L, Hylton N, Yassa L, et al. Utility of Magnetic Resonance Imaging in the management of breast cancer: evidence for improved preoperative staging. *J Clin Oncol*. 1999; 17:110–119. [PubMed: 10458224]

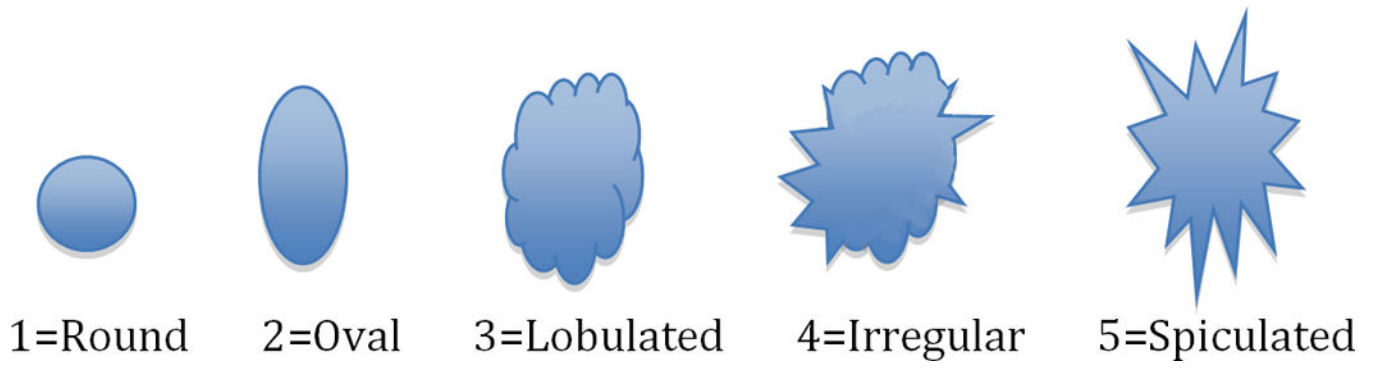


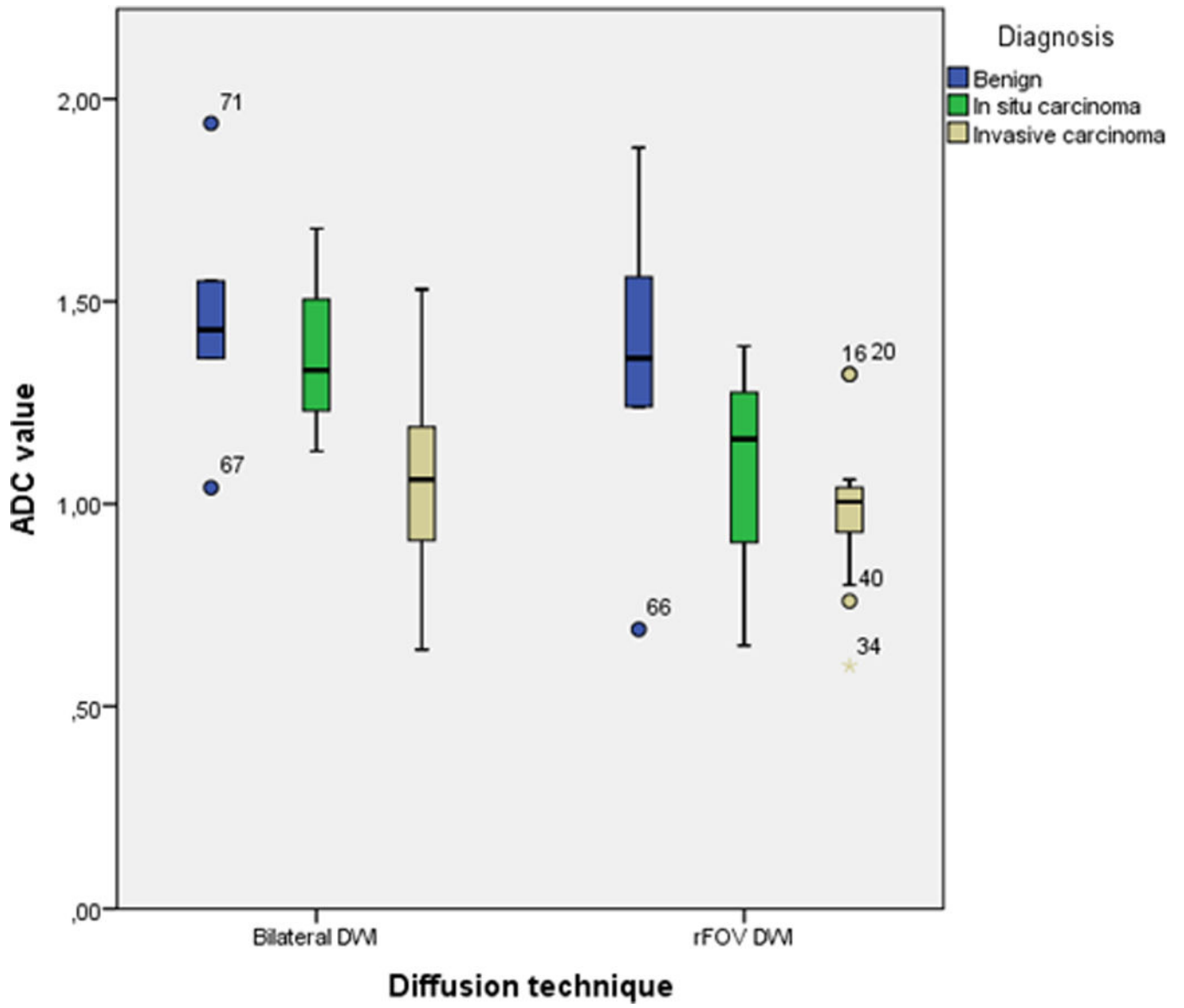
Figure 1.
Lesion interpretation on the basis of different lesion shapes

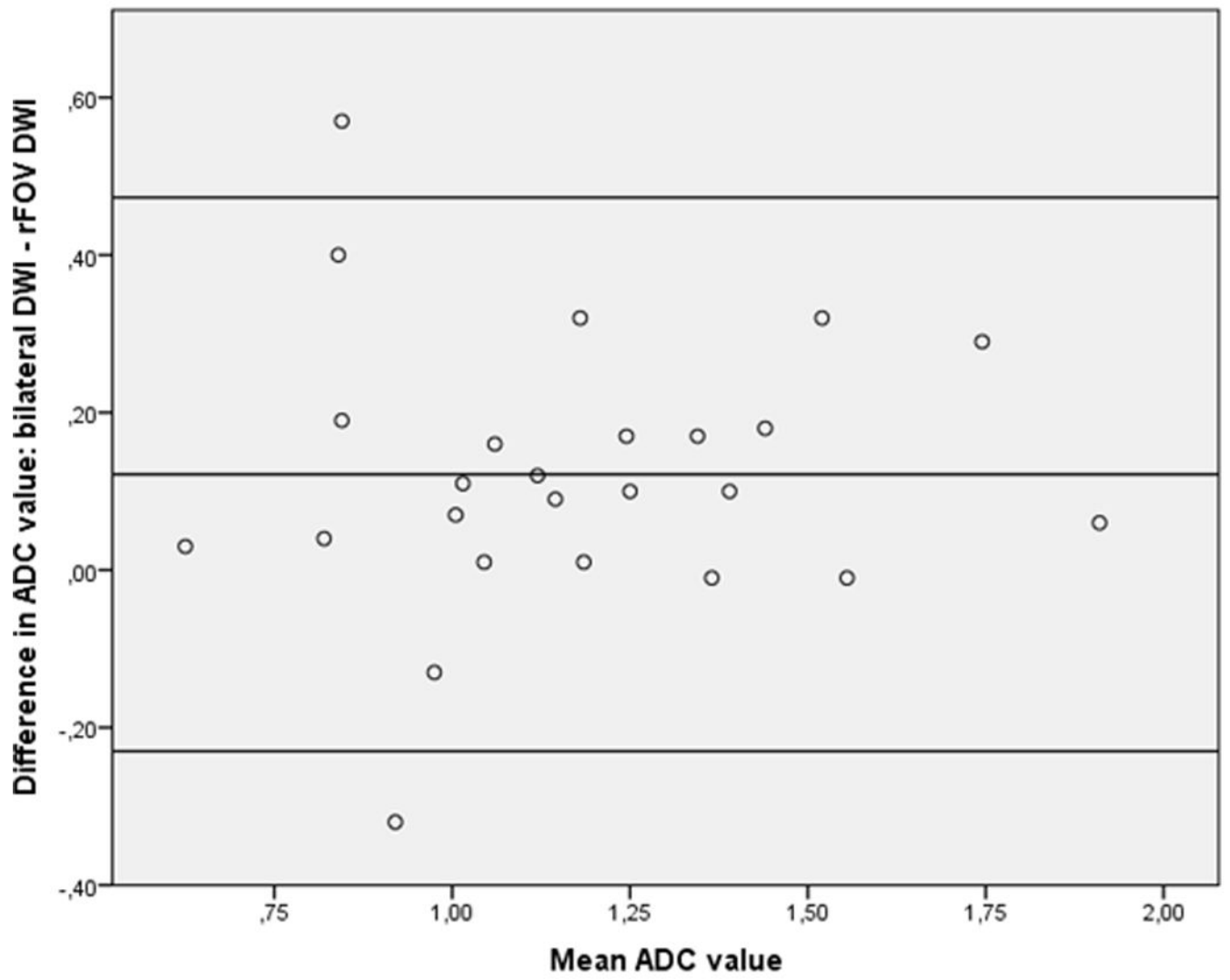
Author Manuscript

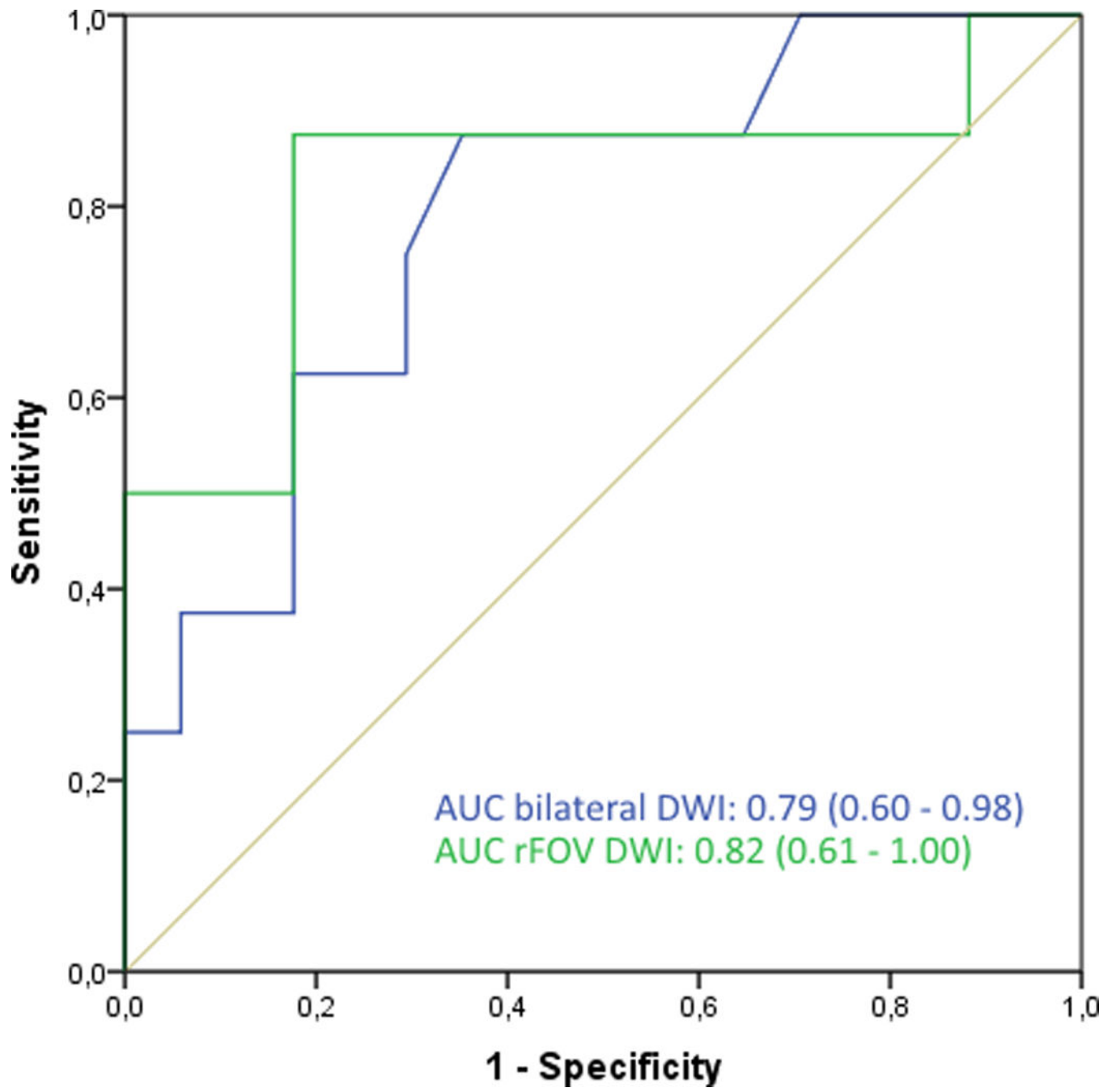
Author Manuscript

Author Manuscript

Author Manuscript







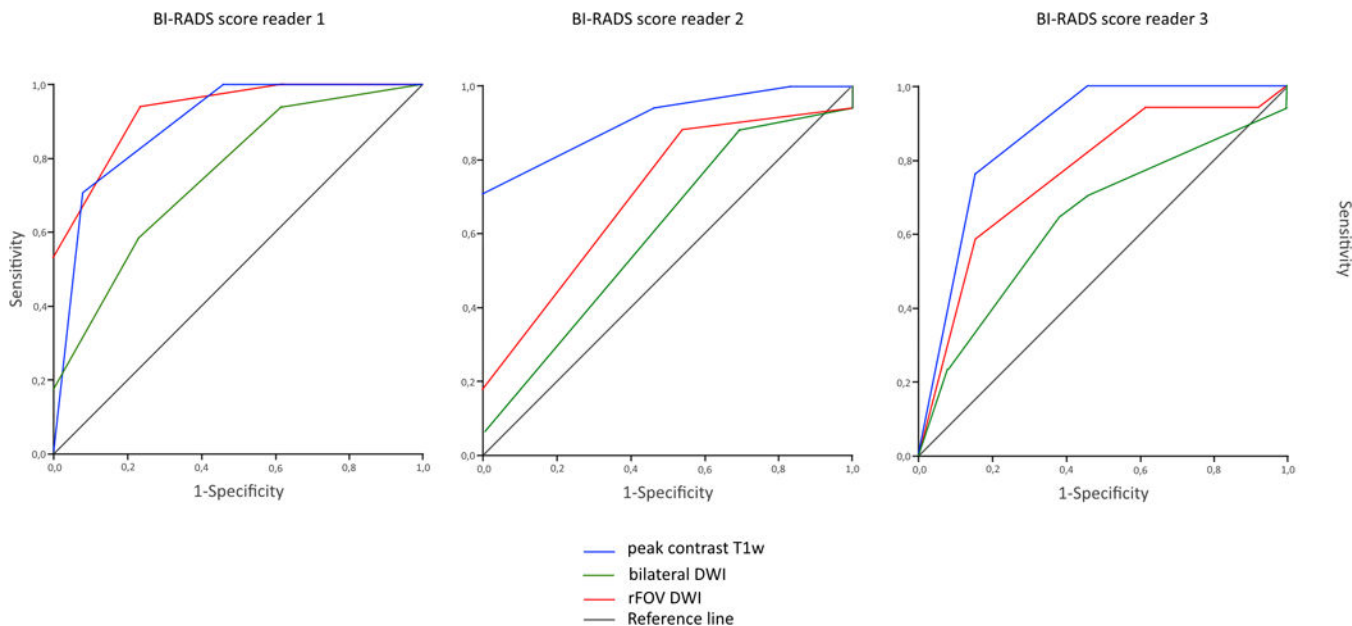


Figure 2.

- a.** Boxplot showing the ADC values, comparing bilateral DWI and rFOV DWI categorized by diagnosis.
 - b.** Bland Altman plot showing difference in ADC value (bilateral DWI – rFOV DWI) versus mean ADC value
 - c.** ROC curves, showing the discriminative abilities of bilateral and rFOV DWI based on ADC values
 - d.** ROC curves, showing the discriminative abilities of the readers based on BI-RADS classification on peak contrast T1w images, bilateral DWI, and rFOV DWI
- Corresponding AUC values were

Reader 1:	peak contrast T1w	: 0.89 (0.77–1.00)
	bilateral DWI	: 0.76 (0.58–0.93)
	rFOV DWI	: 0.93 (0.84–1.00)
Reader 2:	peak contrast T1w	: 0.91 (0.80–1.00)
	bilateral DWI	: 0.61 (0.40–0.81)
	rFOV DWI	: 0.71 (0.52–0.90)
Reader 3:	peak contrast T1w	: 0.87 (0.73–1.00)
	bilateral DWI	: 0.64 (0.44–0.84)
	rFOV DWI	: 0.76 (0.59–0.94)

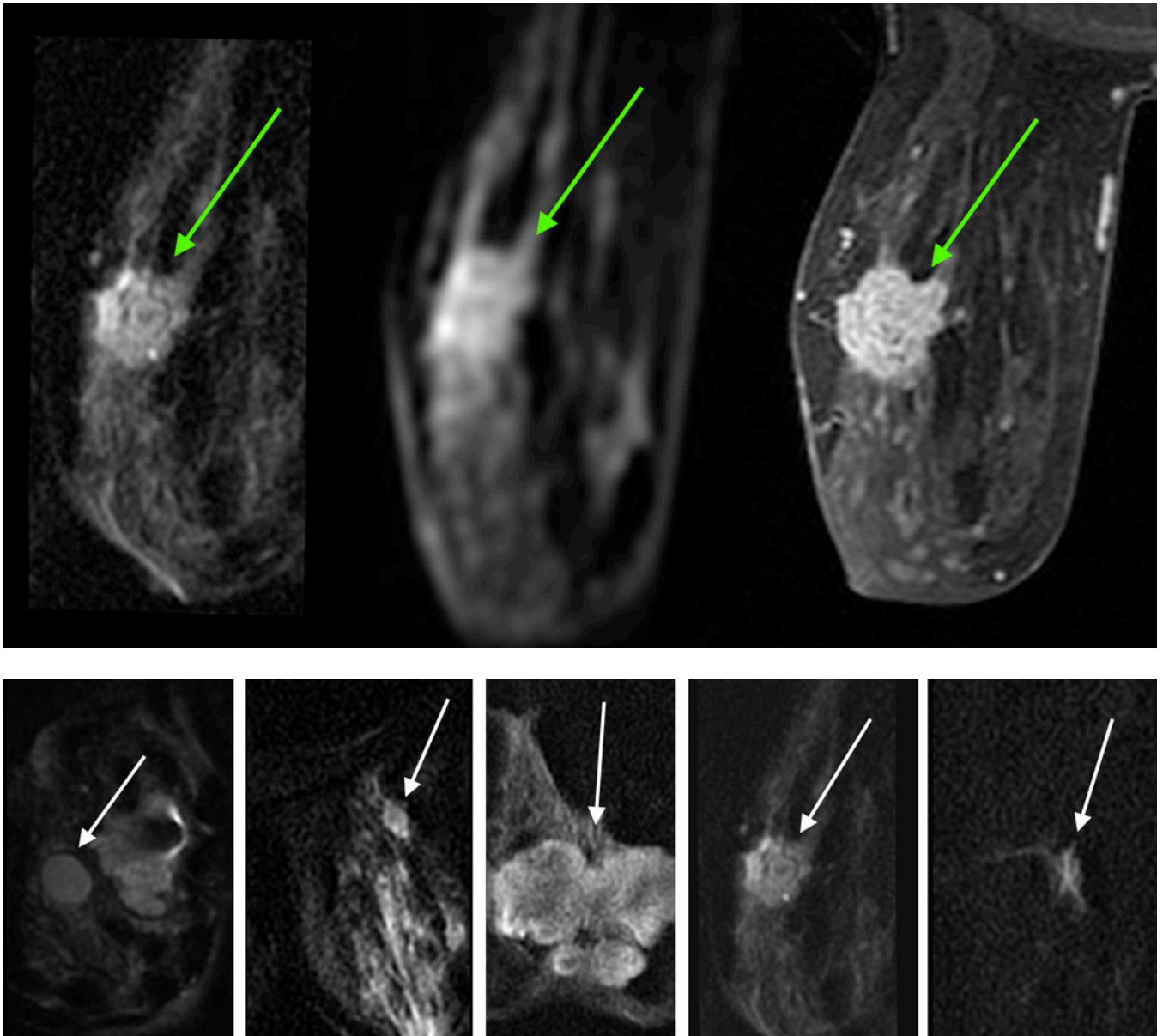


Figure 3.
a. 70-year-old woman with a grade 3 invasive ductal carcinoma (arrow)
b. Example of lesions on rFOV DWI according to the classification of Figure 1.

Table 1

Phantom relaxation times and ADC values in NIST breast phantom

	T1** relaxation time (ms)	T2** relaxation time (ms)	Reference* ADC (mm²/s)	Bilateral DWI ADC (mm²/s)	rFOV DWI ADC (mm²/s)
10% PVP	2021 ± 63.5	1120 ± 449.1	1.8	1.630.03	1.690.1
25% PVP	1033 ± 12.1	471 ± 138.1	1.0	0.940.02	0.990.1
40% PVP	625 ± 10.5	465 ± 209.1	0.65	0.540.02	0.610.09

Abbreviations: ADC: apparent diffusion coefficient; SD: standard deviation; NIST: National Institute of Standards and Technology; PVP: polyvinylpyrrolidone; DWI: diffusion-weighted imaging; rFOV: reduced field-of-view.

* measurement performed at 20.5°C

** T1/T2 values provided by the phantom manufacturer

Table 2

Patients' and lesions' characteristics

Total patients: 21	N (%)
Female	21 (100)
Mean age in years \pm SD (range)	51.3 \pm 9.1 (41–70)
Indication for MRI	
<i>Staging</i>	15 (71.4)
<i>Diagnostic for unclear finding</i>	6 (28.6)
Total lesions: 30	
Lesion size in centimeters (mean \pm SD)	2.63 \pm 2.04
Range	0.6 – 8.5
Background enhancement	
<i>No</i>	1 (3.3)
<i>Minimal</i>	11 (36.7)
<i>Mild</i>	3 (10.0)
<i>Moderate</i>	6 (20.0)
<i>Marked</i>	9 (30.0)
Initial type of pathology	
<i>CNB</i>	24 (80.0)
<i>Imaging / No biopsy</i>	5 (16.7)
<i>Mastectomy for other lesion</i>	1 (3.3)
Clip present	
<i>Yes</i>	15 (50.0)
<i>No</i>	15 (50.0)
Initial diagnosis category	
<i>Benign</i>	10 (33.3)
- <i>Cyst</i>	– 5
- <i>Fibrocystic changes</i>	– 2
- <i>UDH</i>	– 1
- <i>Adenosis</i>	– 1
- <i>Fibroadenoma</i>	– 1
<i>High risk</i>	3 (10.0)
- <i>ADH</i>	– 1
- <i>ALH</i>	– 1
- <i>Papilloma</i>	– 1
<i>In situ carcinoma</i>	3 (10.0)
- <i>DCIS</i>	– 3
<i>Invasive carcinoma</i>	14 (46.7)
- <i>IDC</i>	– 14
Invasive breast cancer grade	
<i>Nottingham grade 1</i>	2 (14.3)
<i>Nottingham grade 2</i>	4 (28.6)

Total patients: 21	N (%)
<i>Nottingham grade 3</i>	8 (57.1)
Associated DCIS with invasive carcinoma	
<i>Yes</i>	11 (78.6)
<i>No</i>	3 (21.4)
ER status	
<i>Positive</i>	9 (56.3)
<i>Negative</i>	6 (37.5)
<i>Unknown</i>	1 (6.3)
PR status	
<i>Positive</i>	8 (50.0)
<i>Negative</i>	7 (43.8)
<i>Unknown</i>	1 (6.3)
HER2-Neu status	
<i>Positive</i>	2 (13.3)
<i>Negative</i>	11 (73.3)
<i>Unknown</i>	2 (13.3)

Abbreviations: SD: standard deviation; MRI: magnetic resonance imaging; CNB: core needle biopsy; UDH: usual type ductal hyperplasia; DCIS: ductal carcinoma *in situ*; IDC: invasive ductal carcinoma; ER: estrogen receptor; PR: progesterone receptor; HER2-Neu: human epidermal growth factor receptor 2.

Table 3

Results of the image quality assessment, comparing bilateral DWI with rFOV DWI rated by three observers

Image Quality	Reader 1		Reader 2		Reader 3	
	Bilateral DWI	rFOV DWI	Bilateral DWI	rFOV DWI	Bilateral DWI	rFOV DWI
Sharpness						
1=unsharp	5	0	0	1	4	1
2=somewhat unsharp	15	2	21	4	17	9
3=moderately sharp	1	10	0	7	0	4
4=sharp	0	7	0	9	0	5
5=very sharp	0	2	0	0	0	2
	$P<0.001$		$P<0.001$		$P=0.002$	
Artifacts/ghosting						
0=no artifacts	4	13	3	1	6	12
1=some, but interpretable	14	8	11	15	10	8
2=severe, but interpretable	3	0	5	5	4	1
3=severe, interpretation problems	0	0	2	0	1	0
	$P=0.003$		$P=0.614$		$P=0.056$	
Distortions						
0=no distortions	8	17	6	7	16	21
1=some, but interpretable	12	4	14	12	4	0
2=severe, but interpretable	1	0	1	2	1	0
3=severe, interpretation problems	0	0	0	0	0	0
	$P=0.004$		$P=1.00$		$P=0.034$	
Perceived signal to noise						
1=poor	2	1	0	0	0	0
2=acceptable	11	2	7	13	6	2
3=good	7	11	14	8	15	11
4=excellent	1	7	0	0	0	8
	$P<0.001$		$P=0.058$		$P=0.005$	

Image Quality	Reader 1		Reader 2		Reader 3	
	Bilateral DWI	rFOV DWI	Bilateral DWI	rFOV DWI	Bilateral DWI	rFOV DWI
Fat suppression						
1=failed	0	0	0	0	1	0
2=poor	1	0	3	0	1	0
3=acceptable	7	4	12	15	7	0
4=good	13	17	6	6	12	12
5=excellent	0	0	0	0	0	9
	$P=0.059$		$P=0.417$		$P=0.002$	

* $P<0.05$, Wilcoxon signed-rank test

Abbreviations: DWI: diffusion-weighted imaging; rFOV: reduced field of view

Table 4

Interrater agreement and reliability on BI-RADS classification

		Reader 1–2	Reader 1–3	Reader 2–3
Post-contrast	Proportion of agreement	56%	82%	56%
T1w	Reliability (weighted kappa)	0.51	0.83	0.51
Bilateral DWI	Proportion of agreement	47%	47%	38%
	Reliability (weighted kappa)	0.33	0.50	0.21
rFOV DWI	Proportion of agreement	41%	59%	41%
	Reliability (weighted kappa)	0.32	0.61	0.38

Abbreviations: DWI: diffusion-weighted imaging; rFOV: reduced field of view